

Color Image Quality Metric S-CIELAB and Its Application on Halftone Texture Visibility

Xuemei Zhang
Department of Psychology
Stanford University
Stanford, CA 94305
xmei@psych.stanford.edu

D. Amnon Silverstein, Joyce E. Farrell
Hewlett Packard Laboratories
1501 Page Mill Road
Palo Alto, CA 94304
amnon@hpl.hp.com, joyce@hpl.hp.com

Brian A. Wandell
Department of Psychology
Stanford University
Stanford, CA 94305
brian@white.stanford.edu

Abstract

We describe experimental tests of a spatial extension to the CIELAB color metric for measuring color reproduction errors of digital images. The standard CIELAB ΔE metric is suitable for use on large uniform color targets, but not on images, because color sensitivity changes as a function of spatial pattern. The S-CIELAB extension includes a spatial processing step, prior to the CIELAB ΔE calculation, so that the results correspond better to color difference perception by the human eye.

The S-CIELAB metric was used to predict texture visibility of printed halftone patterns. The results correlate with perceptual data better than standard CIELAB and point the way to various improvements.

1. Introduction

In digital color imaging applications, it is often necessary to evaluate the visibility of color reproduction errors. The decision to proceed or not with a hardware modification can depend on the predicted color reproduction error caused by the hardware change.

To measure perceptual color differences between two color images, we must account for several aspects of human visual sensitivity. First, human sensitivity to color differences is not uniform in linear color spaces such as the CIE XYZ color space [9]. Distance between two colors in a linear color space does not correspond

to perceptual differences between them.

Second, sensitivity to color differences depends on the color of the background or adaptation state of the eye, which can be changed by ambient illumination [1, 17, 8, 15].

Third, sensitivity to color differences also depends on spatial pattern [2, 10, 11, 12].

These are all significant visual effects. There has been theoretical work on incorporating each of these factors into modern color metrics.

The CIELAB transformation incorporates the fact that perceptual differences among colors are not uniform in a linear color space. This metric is widely used in industry to measure color reproduction errors [6, 7, 3]. The CIELAB metric transforms colors to a representation which is approximately perceptually uniform in the sense that Euclidean distances between different colors in this space correspond roughly to perceived color differences. The CIELAB transformation is based on data from color matching and discrimination experiments using large uniform test fields under fixed adaptation condition. While imperfect, it works reasonably well in applications involving large uniform patches viewed under standard illuminants.

The effects of visual adaptation are partially included in the original CIELAB metric. However, the standard CIELAB calculations do not explain performance well (e.g. Wandell and Brainard [16]). Fairchild and Berns [5]) have proposed a set of computations to improve on the original CIELAB definitions.

Here, we will discuss a spatial extension to the

CIELAB color metric called S-CIELAB [18], and its application on predicting halftone pattern visibility.

2. S-CIELAB model

Zhang and Wandell [18] proposed a spatial extension to CIELAB to account for how spatial pattern influences color appearance and color discrimination. The spatial extension is accomplished by pre-processing the input images before applying standard CIELAB color difference formula. An input image is initially converted into one luminance and two chrominance color components. Each component image is then passed through a spatial filter that is selected according to the spatial sensitivity of the human eye for that color component. The final filtered images are transformed into XYZ format so that the standard CIELAB color difference formula can be applied.

Consistent with the perceptual measurements, and to make the spatial filtering calculations efficient, Zhang and Wandell used a pattern-color separable architecture (Poirson and Wandell [11, 12]).

The spatial filtering is performed in a linear color space using unit sum filters; consequently the spatial filtering preserves mean color values of an input image. Hence, for large uniform targets, the S-CIELAB predictions are the same as the CIELAB predictions. For textured regions, however, the two formulae can make very different predictions.

3. Application: Halftone pattern visibility

In this paper we consider one of many potential applications of the S-CIELAB metric - halftone visibility in printed images. To perform these experiments, we required

1. A method for evaluating the visibility of printed halftone texture by human subjects.
2. A method for computing S-CIELAB metric on printed images.

We used printed halftone swatches with different colors and texture patterns as experimental stimuli. We obtained perceptual texture visibility data from human subjects, and computed S-CIELAB predictions of texture visibility for these halftone patches. S-CIELAB predictions were compared with the empirical data. The S-CIELAB measures halftone texture visibility somewhat more accurately than standard CIELAB.

3.1. Methods

Apparatus: We measured contrast thresholds for printed halftones using a “pattern strength meter” (PSM), which is a modification of the device described in [13]. The PSM provides a means of optically adjusting the contrast of a spatial test pattern. The experimental stimuli were created by creating convex optical sums of a sharply focused image of the test pattern, f , with an optically blurred image of the test pattern, b . The optical mixtures were of the form $pf + (1 - p)b$, where p is between 0 and 1. The blurred image had essentially zero contrast and thus represented only the mean intensity of the image. The focused image had the same contrast as the original test pattern. Subjects adjusted a knob to control the parameter p and hence the contrast of the stimulus relative to the test pattern. For example, the subject could turn the knob to set $p = 0.1$ and in this way create a stimulus with 1/10 the contrast of the original pattern. The stimulus displayed on the PSM was identical to the original pattern in all respects except that its amplitude relative to its mean was reduced. The stimulus was not a blurred version of the original test pattern.

The stimulus was viewed through a black circular aperture 3.8 degrees in diameter. The effective viewing distance was 8.9 inches.

Stimulus: A total of 17 halftone test patterns were used in the experiment. We chose the halftone stimuli so that the sample contained a variety of colors and texture styles. The halftone patterns were created using 3 different halftone methods: clustered-dot, Bayer, and error diffusion. Eight of the 17 patches were halftoned using black and white dots, five using red and green dots, and four using blue and yellow dots. The halftone patterns were printed on a Kodak dye-sublimation printer. The printing resolution was 150 dpi for the Bayer and error diffusion halftone patterns, and 300 dpi for the clustered-dot halftone patterns.

Stimulus calibration: We needed accurate digital representations of the printed halftone images in calibrated XYZ format in order to perform S-CIELAB calculations on them. To calibrate the stimuli, we scanned the halftone patches on a high resolution color scanner (Agfa Horizon, 1200 dpi optical resolution) and transformed the scanned RGB images into XYZ format.

Because the scanner RGB sensors’ spectral sensitivities were not linear transformations of the XYZ color matching functions, R,G,B images obtained from one scan on the scanner do not contain enough information to be correctly transformed into XYZ images. We dealt

with this problem by performing 3 additional scans for each target, each time putting a different color plastic filter underneath the target. The color filters effectively changed the spectral sensitivities of the scanner’s sensors. Therefore, by combining the 4 sets of R,G,B color component images obtained from the standard scan and the 3 filtered scans, we can get a more accurate transformation into XYZ format. The transformation matrix was solved by scanning a panel of calibrated color patches with known XYZ values (if viewed under the same Tungsten light illumination as in the experiment). Thus, we effectively have an XYZ scanner by using the above scanning procedures and then performing the appropriate transformations on the scanned data.

We compared the XYZ values for solid color patches measured with the scanner and the XYZ values measured with a colorimeter. For averages over a 0.3x0.3 inch solid color area, the scanned XYZ values differ from the colorimeter XYZ values by about 5 ΔE units. A large portion of these errors come from unreliable Z values. The X and Y values obtained from the scanner were much more accurate than the Z values. Since the light source in the scanner is a Tungsten-Halogen lamp, which has relatively low energy at the short wavelength side, the unreliable estimates of Z values (which represent short wavelength components of the input image) are understandable.

The overall accuracy of the XYZ scanning procedure was considered adequate for the purpose of this study.

All of the 17 halftone patches were scanned into XYZ format at 1200 dpi using the scanning procedure described above.

Subjects: Subjects were 5 employees in Hewlett Packard Laboratories. Three of them were female, and two of them were male. All subjects had normal or corrected-to-normal visual acuity and normal color vision.

Procedures: Subjects viewed the set of test patterns through the PSM in a randomized sequence. They adjusted the pattern contrast until the texture was just visible, and the experimenter recorded the final *p* level. The pattern and the subject were illuminated with the same tungsten light source so the subject remained adapted to the same source that illuminated the pattern. Each subject completed at least one setting for each halftone test patch. Some subjects completed more than one settings per patch. A total of 11 settings were collected for each halftone test patch.

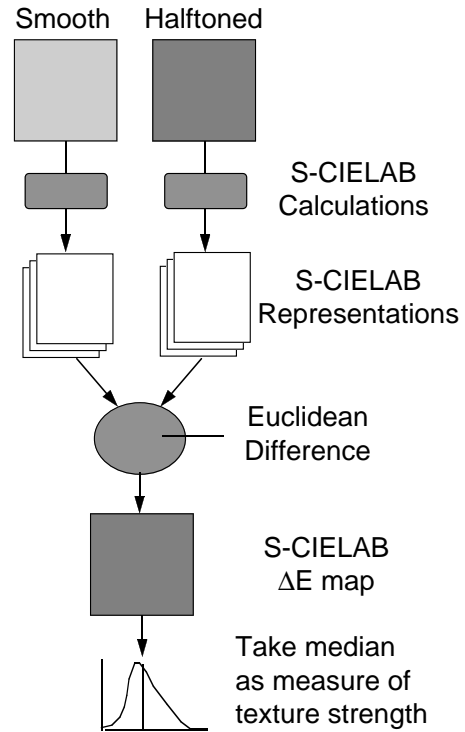


Figure 1. Steps of calculations when using S-CIELAB as a metric for halftone texture visibility.

Model fits: We used the scanned XYZ representations of each halftone patch to predict its visibility. For the S-CIELAB predictions, we compared each halftoned image with a uniform field that had the same mean as the halftone. The S-CIELAB calculations provide a ΔE value that compares each pixel in the original halftone patch and a corresponding pixel in the uniform patch. We used the median of these ΔE values as an overall indicator of the visibility of the halftone image. The computational steps are illustrated in Figure 1.

To predict the experimental settings for each pattern, we computed the level p of the halftone mixture that reduced the median S-CIELAB ΔE difference between the mixture and the uniform field was exactly 0.5. Thus, a median ΔE value of 0.5 was defined as the visibility threshold in the S-CIELAB model. We plot the measured *visibility* of the pattern, $1/p$, against the predicted values. Predictions for the CIELAB color difference metric were generated in a similar way.

3.2. Results

Figure 2 shows the predicted and observed visibility for the various halftone patterns. Visibility data obtained from human subjects are plotted against the CIELAB predictions (bottom plot) correlate poorly with the perceptual visibility data (linear $R^2 = 0.075$); the data do not have any obvious monotonic increasing trend. Notice that the CIELAB visibility of the black-white points (asterisks) do correlate well with the perceptual visibility data ($R^2 = 0.74$). However, CIELAB over-estimates the texture visibility of halftone patterns composed of red-green dots or blue-yellow dots. This is not surprising since for high spatial frequency targets, visual sensitivity to chromatic contrast is much lower than sensitivity to luminance contrast. Standard CIELAB does not take this into account, and therefore tend to over-estimate visibility of chromatic texture patterns.

The S-CIELAB predictions (top plot) correlates somewhat better with the perceptual visibility data (linear $R^2 = 0.46$). The S-CIELAB visibility estimates for black-white patterns still correlate well with the perceptual visibility values ($R^2 = 0.89$). Visibility estimates of chromatic texture patterns are comparable to black-white patterns, except that the data points representing chromatic texture patterns are more variable.

While the S-CIELAB predictions are better than those of CIELAB, there are still significant deviations. We are aware of several reasons for these errors. First, the basic CIELAB predictions for color discrimination are imperfect and any CIELAB imperfections will be

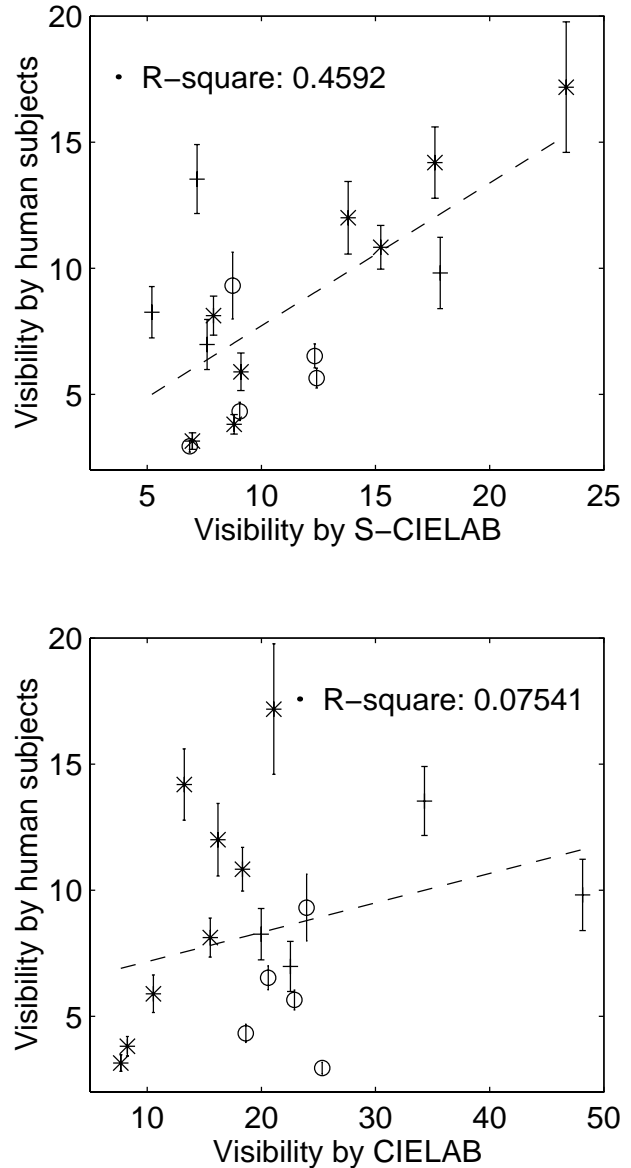


Figure 2. Perceptual texture visibility of printed halftone patterns plotted against (a) visibility measured by S-CIELAB (top) and (b) visibility measured by CIELAB (bottom). Data points shown as asterisk symbols correspond to patterns halftoned with black and white dots; circles correspond to patterns halftoned with red and green dots; pluses correspond to patterns halftoned with blue and yellow dots. The data points should fall on a straight line if the model's predictions correlate perfectly with the experimental data. The R^2 values of the best-fitting straight lines are shown in the plots.

inherited by S-CIELAB. Second, S-CIELAB does not include any provisions for masking or orientation specific effects. Third, there were small but systematic errors in the image calibration. Specifically, there was considerable error in our estimates of the tristimulus value of Z. As a result, we see much higher variance in visibility predictions by both S-CIELAB and CIELAB for the blue-yellow halftone patterns, than for the black-white and red-green halftone patterns.

4. Further Developments

Our measurements of halftone visibility on printed media, showed that (a) S-CIELAB predictions represent a significant improvement over CIELAB, and (b) there is room for more improvement. The two principal directions we believe should be explored are the effects of visual pattern masking and multiresolution representations (e.g., [14, 4]).

5. Conclusions

The S-CIELAB calculation extends CIELAB by incorporating factors related to the pattern-color sensitivities of the human eye. It can be used to measure color differences in digital images. S-CIELAB can be used to improve predictions concerning the visibility of halftone textures.

References

- [1] C. Bartleson. A review of chromatic adaptation. *AIC Proceedings in Color 77, Troy*, pages 63–96, 1978.
- [2] H. Bäuml and B. Wandell. The color appearance of mixture gratings. *Vision Research*, 99(7):1–100, 1996.
- [3] R. Berns. Deriving instrumental tolerances from pass-fail and colorimetric data. *Color Research and Applications*, 21(6):459–472, December 1996.
- [4] S. Daly. Quantitative performance assessment of an algorithm for the determination of image fidelity. *SID Digest*, pages 317–320, 1993.
- [5] M. D. Fairchild and R. S. Berns. Image color-appearance specification through extension of cielab. *Color Research and Application*, 18(3):178–190, June 1993.
- [6] International Commission on Illumination. Recommendations on uniform color spaces, color difference equations, psychometric color terms. *Supplement No.2 to CIE publication No.15 (E.-1.3.1)*, TC-1.3., 1971.
- [7] International Commission on Illumination. Industrial colour-difference evaluation. 1995.
- [8] P. Lennie and M. D’Zmura. Mechanisms of color vision. *CRC Critical Review of Neurobiology*, 3:333–400, 1988.
- [9] D. MacAdam. Visual sensitivities to color differences in daylight. *Journal of the Optical Society of America*, 32:247–274, 1942.
- [10] C. Noorlander and J. Koenderink. Spatial and temporal discrimination ellipsoids in color space. *Journal of the Optical Society of America*, 73:1533–1543, 1983.
- [11] A. Poirson and B. Wandell. Appearance of colored patterns: pattern-color separability. *Journal of the Optical Society of America*, 10(12):2458–2470, 1993.
- [12] A. Poirson and B. Wandell. Pattern-color separable pathways predict sensitivity to simple colored patterns. *Vision Research*, 35(2):239–254, 1996.
- [13] D. A. Silverstein and J. E. Farrell. The relationship between image fidelity and image quality. *Proceedings of the 1996 ICIP, IEEE*, 1996.
- [14] P. C. Teo and D. J. Heeger. Perceptual image distortion. *First International Conference on Image Processing*, 2:982–986, November 1994.
- [15] J. von Kries. Chromatic adaptation. *Festschrift der Albrecht-Ludwig-Universität, Fribourg*, 1902.
- [16] B. Wandell and D. Brainard. Towards cross-media color reproduction. *Applied Vision 1989 Tech Digest Series*, 16(7):132–137, July 12-14 1989.
- [17] W. Wright. Why and how chromatic adaptation has been studied. *Color Research and Application*, 6:147–152, 1981.
- [18] X. M. Zhang and B. A. Wandell. A spatial extension to CIELAB for digital color image reproduction. *Symposium Proceedings*, 1996.